



**HAL**  
open science

## Synthesis and Neurotoxicity Profile of 2,4,5-Trihydroxymethamphetamine and Its 6-( N -Acetylcystein- S -yl) Conjugate

Anne Neudörffer, Melanie Mueller, Claire-Marie Martinez, Annis Mechan,  
Una Mccann, George Ricaurte, Martine Largeron

► **To cite this version:**

Anne Neudörffer, Melanie Mueller, Claire-Marie Martinez, Annis Mechan, Una Mccann, et al.. Synthesis and Neurotoxicity Profile of 2,4,5-Trihydroxymethamphetamine and Its 6-( N -Acetylcystein- S -yl) Conjugate. *Chemical Research in Toxicology*, 2011, 24 (6), pp.968-978. 10.1021/tx2001459 . hal-02384825

**HAL Id: hal-02384825**

**<https://hal.science/hal-02384825>**

Submitted on 5 Feb 2021

**HAL** is a multi-disciplinary open access archive for the deposit and dissemination of scientific research documents, whether they are published or not. The documents may come from teaching and research institutions in France or abroad, or from public or private research centers.

L'archive ouverte pluridisciplinaire **HAL**, est destinée au dépôt et à la diffusion de documents scientifiques de niveau recherche, publiés ou non, émanant des établissements d'enseignement et de recherche français ou étrangers, des laboratoires publics ou privés.

Published in final edited form as:

*Chem Res Toxicol.* 2011 June 20; 24(6): 968–978. doi:10.1021/tx2001459.

## Synthesis and Neurotoxicity Profile of 2,4,5-Trihydroxymethamphetamine and its 6-(*N*-Acetylcystein-*S*-yl) Conjugate

Anne Neudörffer<sup>†</sup>, Melanie Mueller<sup>‡</sup>, Claire-Marie Martinez<sup>†</sup>, Annis Mehan<sup>‡</sup>, Una McCann<sup>§</sup>, George A. Ricaurte<sup>\*‡</sup>, and Martine Langeron<sup>\*†</sup>

<sup>†</sup> UMR 8638 CNRS - Université Paris Descartes, Synthèse et Structure de Molécules d'Intérêt Pharmacologique, Faculté des Sciences Pharmaceutiques et Biologiques, 4 Avenue de l'Observatoire, 75270 Paris cedex 06, France

<sup>‡</sup> Department of Neurology, Johns Hopkins University School of Medicine, 5501 Hopkins Bayview Circle, Baltimore, Maryland 21224

<sup>§</sup> Department of Psychiatry and Behavioral Sciences, Johns Hopkins University School of Medicine, 5501 Hopkins Bayview Circle, Baltimore, Maryland 21224

### Abstract

The purpose of the present study was to determine if trihydroxymethamphetamine (THMA), a metabolite of methylenedioxyamphetamine (MDMA, “ecstasy”) or its thioether conjugate, 6-(*N*-acetylcystein-*S*-yl)-2,4,5-trihydroxymethamphetamine (6-NAC-THMA), plays a role in the lasting effects of MDMA on brain serotonin (5-HT) neurons. To this end, novel high-yield syntheses of THMA and 6-NAC-THMA were developed. Lasting effects of both compounds on brain serotonin (5-HT) neuronal markers were then examined. A single intraventricular injection of THMA produced a significant lasting depletion of regional rat brain 5-HT and 5-hydroxyindoleacetic acid (5-HIAA), consistent with previous reports that THMA harbors 5-HT neurotoxic potential. The lasting effect of THMA on brain 5-HT markers was blocked by the 5-HT uptake inhibitor fluoxetine, indicating persistent effects of THMA on 5-HT markers, like those of MDMA, are dependent on intact 5-HT transporter function. Efforts to identify THMA in the brains of animals treated with a high, neurotoxic dose (80 mg/kg) of MDMA were unsuccessful. Inability to identify THMA in brains of these animals was not related to the unstable nature of the THMA molecule, because exogenous THMA administered intracerebroventricularly could be readily detected in the rat brain for several hours. The thioether conjugate of THMA, 6-NAC-THMA, led to no detectable lasting alterations of cortical 5-HT or 5-HIAA levels, indicating that it lacks significant 5-HT neurotoxic activity. The present results cast doubt on the role of either THMA or 6-NAC-THMA in the lasting serotonergic effects of MDMA. The possibility remains that different conjugated forms of THMA, or oxidized cyclic forms (e.g. the indole of THMA) play a role in MDMA-induced 5-HT neurotoxicity *in vivo*.

\*CORRESPONDING AUTHOR: Tel:(+) 33 1 53 73 96 46; Fax: (+) 33 1 44 07 35 88, martine.langeron@parisdescartes.fr; ricaurte@jhmi.edu.

Supporting Information Available. <sup>1</sup>H and <sup>13</sup>C NMR spectra of THMA and its synthetic intermediates, together with 6-(*N*-acetylcystein-*S*-yl)-THMA; analytical HPLC chromatograms of THMA and of 6-(*N*-acetylcystein-*S*-yl)-THMA. This information is available free of charge via the Web at <http://pubs.acs.org>.

## Introduction

3,4-Methylenedioxymethamphetamine (MDMA, “ecstasy”) is a drug of abuse that produces lasting decreases in various pre-synaptic serotonergic neuronal markers including 5-HT, its major metabolite, 5-hydroxyindoleacetic acid (5-HIAA), its biosynthetic enzyme, tryptophan hydroxylase (TPH) and its membrane re-uptake site, the 5-HT transporter (SERT) (1,2). These decrements in 5-HT axonal markers are accompanied by anatomical signs of 5-HT axonal damage (3,4) and a lasting decrease in anterograde [<sup>3</sup>H]proline transport from the dorsal raphe nucleus to the forebrain (5). Collectively, these lasting chemical and anatomical alterations after MDMA exposure have been widely interpreted as being indicative of a toxic effect of MDMA on brain 5-HT axon terminals (1, 2, 6). Such neurotoxic effects of MDMA have been documented in a variety of species, including non-human primates. In most species (including primates), MDMA selectively damages brain 5-HT neurons (1, 2, 7). For uncertain reasons, in mice, MDMA selectively damages brain dopamine (DA) neurons (8). Despite knowledge of MDMA’s neurotoxic properties for more than two decades (9), the mechanisms by which MDMA damages brain axons and axon terminals are not known (2, 10).

Research demonstrating that central administration of MDMA fails to produce 5-HT neurotoxicity (11–14) has led to the suspicion that systemic metabolism of peripherally administered MDMA is required for the expression of neurotoxicity. This suspicion has generally been taken to suggest that a toxic metabolite is responsible for the lasting effects of MDMA on brain 5-HT neurons. In this regard, thioether conjugates of MDMA metabolites have drawn particular attention (15–18).

Of various potentially toxic metabolites of MDMA (Scheme 1), recent evidence indicates that several metabolites do not appear to be directly involved. These include 3,4-dihydroxymethamphetamine (HHMA) (14, 19, 20) and 4-hydroxy-3-methoxymethamphetamine (HMMA) (20), both of which are phase I and phase II metabolites generated through *O*-demethylenation, and 3,4-dihydroxyamphetamine (HHA) (21), which is produced *via N*-demethylation followed by *O*-demethylenation. In particular, exposure to these metabolites does not result in lasting 5-HT deficits. More recently, the thioether conjugate of HHMA, 5-(*N*-acetylcystein-*S*-yl)-HHMA (5-NAC-HHMA) has been implicated in MDMA neurotoxicity (18) but efforts to replicate these findings have been unsuccessful (20).

One metabolite of MDMA that has not yet been excluded as the mediator of MDMA neurotoxicity is 2,4,5-trihydroxymethamphetamine (THMA) (23, 24). This metabolite, arising from the ring hydroxylation biotransformation step (Scheme 1), is a particularly intriguing candidate because it has structural similarity to the well known DA neurotoxin, 6-hydroxydopamine (6-OHDA), has been reported to be formed endogenously in the liver (22), and has already been shown to produce lasting 5-HT deficits when administered centrally (23, 24). Of note, however, THMA has never been detected in the brains of animals treated with MDMA.

Although extensive work has been done with thioether conjugates of HHMA (18, 20, 25–28), there are no published reports on thioether conjugates of THMA. Notably, thioether conjugates of 6-OHDA have been detected in brains of rats and mice given 6-OHDA centrally (29), suggesting that similar processes may occur with THMA. To our knowledge, synthesis of the thioether conjugate of THMA has yet to be reported.

The goal of the present investigation was to accomplish high-yield syntheses of THMA **4** and its thioether conjugate, 6-(*N*-acetylcystein-*S*-yl)-2,4,5-trihydroxymethamphetamine (6-NAC-THMA) **5** (Scheme 1), and to determine if either of these MDMA metabolites plays a

role in MDMA neurotoxicity. In particular, after confirming earlier findings that centrally administered THMA produces lasting effects on brain 5-HT neurons (23, 24), we sought to: 1) determine if the lasting effect of THMA on 5-HT can be blocked with a 5-HT transporter blocker, fluoxetine, which is known to protect against MDMA neurotoxicity (30); 2) employ newly developed liquid chromatographic-mass spectrometric (LC-MS) methods to ascertain if THMA can be detected in the brains of rats treated with peripherally administered neurotoxic dose of MDMA; 3) test if the inherent instability of the THMA molecule impacts its detectability in brain tissue; and 4) determine if the thioether conjugate of THMA, 6-NAC-THMA **5**, produces lasting effects on brain 5-HT neuronal markers. The present results cast doubt on the role of THMA and its thioether conjugate, 6-NAC-THMA, in MDMA neurotoxicity.

## Experimental Procedures

### Chemical

All reagents and solvents (HPLC grade) were commercial products of the highest available purity and were used as supplied.

Analytical thin-layer chromatography was carried out on silica gel Macherey-Nagel Polygram SIL G/UV 254 (0.25 mm). Column chromatography was performed on Macherey-Nagel Si 60 M silica gel (40–63  $\mu\text{m}$ ). Melting points were measured on a Köfler apparatus.

HPLC was carried out using a Waters system consisting of a 600E multisolvent delivery system, a Rheodyne-type loop injector, and a 2487 dual-channels UV–visible detector set at 254 and 278 nm. A mixture of two solvents A and B constituted the mobile phase. Solvent A was prepared by adding 1% concentrated trifluoroacetic acid (TFA) to deionized water. Solvent B was prepared by adding 0.5% TFA to a 1:1 (v/v) mixture of methanol and deionized water. Semipreparative reversed-phase HPLC was performed using a 250  $\times$  20 mm, 5  $\mu\text{m}$  Kromasil C18 column and a 2 mL loop injector, whereas for the analytical reversed-phase HPLC, a 250  $\times$  4.6 mm, 5  $\mu\text{m}$  Kromasil C18 column, together with a 50  $\mu\text{L}$  loop injector, were used.

$^1\text{H}$  NMR and  $^{13}\text{C}$  NMR spectra were performed on a Bruker AC-300 spectrometer operating at 300 and 75 MHz, respectively. Chemical shifts are expressed as  $\delta$  units (part per million) downfield from TMS (tetramethylsilane). The measurements were carried out using the standard pulse sequences. The carbon type (methyl, methylene, methine, or quaternary) was determined by DEPT experiments.  $^1\text{H}$  and  $^{13}\text{C}$  NMR spectra of all compounds are included in the supporting information as a proof of their identity. High-resolution mass spectra (HRMS) were recorded on a LTQ-Orbitrap spectrometer operating in positive ion mode. UV/vis spectra were recorded on a VARIAN Cary 100 spectrophotometer.

( $\pm$ )-2,4,5-trihydroxymethamphetamine hydrobromide (THMA, HBr) was synthesized in four steps (Scheme 2) from commercially available 2,4,5-trimethoxybenzaldehyde and nitroethane, through a procedure close to those previously reported for the synthesis of ( $\pm$ )-3,4-dihydroxymethamphetamine hydrobromide (HHMA, HBr) with some modifications (31–34).

### 2,4,5-Trimethoxy- $\beta$ -methyl- $\beta$ -nitrostyrene (1)

A solution of 2,4,5-trimethoxybenzaldehyde (2.94 g, 15.0 mmol) and of ammonium acetate (1.18 g, 15.3 mmol) in 60 mL of nitroethane was heated to reflux for 45 min. After evaporation under reduced pressure,  $\text{H}_2\text{O}$  (50 mL) was added to the resulting orange oil, and the reaction mixture was extracted with ethyl acetate (2  $\times$  100 mL). The organic phase was dried over  $\text{MgSO}_4$  and filtered off. Evaporation of the solvent under reduced pressure

afforded **1** in 99.5% (3.77 g, 14.90 mmol) as an orange solid. mp 94–96 °C; (literature (34) mp 93–95 °C) Spectroscopic data were identical to those previously reported (34).

### 2,4,5-trimethoxyphenylacetone (**2**)

Compound **1** (1.52 g, 6.0 mmol) was dissolved at 50 °C in 4.8 mL of toluene. Then, 2.0 g of Fe (36.0 mmol, 6 equiv) (electrolytic powder), 81.1 mg of ferric chloride (0.3 mmol, 0.05 equiv), 19.2 mL of water and 2.1 mL of 35% aqueous solution of HCl (2 equiv) were successively added and the resulting mixture was heated to reflux for 6 h. After filtration through Celite, the residue was washed with ethyl acetate (120 mL). The resulting organic phase was washed with 50 mL of water, dried over MgSO<sub>4</sub>, filtered off and the solvent was evaporated. After column chromatography (toluene/acetone 92.5/7.5), the crude pale yellow solid was recrystallized from diethyl ether affording compound **2** (1.08 g, 4.8 mmol) in 80.5% yield. mp 55–57 °C; <sup>1</sup>H NMR (CDCl<sub>3</sub>) δ 2.15 (s, 3H, CH<sub>3</sub>), 3.63 (s, 2H, CH<sub>2</sub>), 3.81 (s, 3H, OCH<sub>3</sub>), 3.84 (s, 3H, OCH<sub>3</sub>), 3.90 (s, 3H, OCH<sub>3</sub>), 6.55 (s, 1H, H<sub>3</sub>), 6.68 (s, 1H, H<sub>6</sub>). <sup>13</sup>C NMR (CDCl<sub>3</sub>) δ 29.1, 44.8, 56.0, 56.1, 56.5, 97.4, 114.6, 114.8, 142.8, 148.8, 151.5, 207.3. HRMS (ESI) *m/z* calcd for [M + Na]<sup>+</sup> 247.0946; found, 247.0942.

### 2,4,5-trimethoxymethamphetamine (**3**)

To a stirred solution of compound **2** (1.0 g, 4.5 mmol) in dry dichloromethane (10 mL) cooled at –5 °C, was added a 2 M solution of methylamine in THF (10.1 mL, 20.25 mmol, 4.5 equiv). After the reaction mixture was stirred at room temperature for 1h, 1.15 mL of glacial acetic acid (4.5 equiv) was added, followed by sodium *tri*-acetoxyborohydride (Na(AcO)<sub>3</sub>BH) (1.43 g, 6.75 mmol, 1.5 equiv) in small portions. Then, the reaction mixture was stirred at room temperature for 3 h, and quenched with 2.5 M sodium hydroxide aqueous solution (5 mL). The aqueous layer was extracted with diethyl ether (3 × 100 mL) and the combined ether extracts were washed with 2.5 M sodium hydroxide aqueous solution (5 mL) dried over anhydrous MgSO<sub>4</sub>, and evaporated to dryness to give compound **3** as a white solid (1.07 g, 4.5 mmol) in quantitative yield. mp 74–76 °C; <sup>1</sup>H NMR (CDCl<sub>3</sub>) δ 1.01 (d, *J* = 6.0 Hz, 3H), 1.55 (broad s, 1H), 2.36 (s, 3H), 2.52 (m, *J* = 13.0 Hz, 1H), 2.64 (m, *J* = 13.0 Hz, 1H), 2.73 (m, 1H), 3.76 (s, 3H), 3.80 (s, 3H), 3.85 (s, 3H), 6.49 (s, 1H), 6.66 (s, 1H). <sup>13</sup>C NMR (CDCl<sub>3</sub>) δ 19.8, 34.0, 37.5, 55.3, 56.1, 56.3, 56.6, 97.7, 115.1, 119.4, 142.7, 147.9, 151.9. HRMS (ESI) *m/z* calcd for [M + H]<sup>+</sup> 240.1600; found, 240.1594.

### (±)-2,4,5-Trihydroxymethamphetamine hydrobromide (THMA, HBr) (**4**)

THMA was previously described as the hydrochloric salt (24). A 48% aqueous solution of HBr (5.2 mL) (46 mmol) was added to compound **3** (954 mg, 4.0 mmol). The resulting solution was heated to reflux for 2.0 h, under inert atmosphere. After evaporation under reduced pressure, the brown solid was recrystallized successively in dichloromethane-MeOH 90:10 v/v, and chloroform-isopropanol 85:15 v/v mixture, affording THMA, HBr **4** as a white solid (845 mg, 3.04 mmol) in 76% yield. The degree of purity for compound **4** (99%) was determined by analytical HPLC (eluent, solvent A/solvent B 93/7; flow rate, 0.6 mL min<sup>-1</sup>). mp 172–174 °C; UV absorption (0.2 M aqueous HCl) λ<sub>max</sub> = 292 nm, ε = 4300 mol<sup>-1</sup> L cm<sup>-1</sup>. <sup>1</sup>H NMR (D<sub>2</sub>O) δ 1.14 (d, *J* = 6.5 Hz, 3H), 2.57 (s, 3H), 2.69 (m, 2H), 3.37 (m, 1H), 6.38 (s, 1H), 6.60 (s, 1H). <sup>13</sup>C NMR (D<sub>2</sub>O) δ 14.8, 30.1, 32.9, 55.8, 104.2, 113.9, 118.9, 137.1, 143.9, 147.7. Note, when the <sup>1</sup>H NMR spectra of THMA was performed in DMSO D<sub>6</sub>, three additional signals were recorded at 8.09 (1H, OH, D<sub>2</sub>O exchanged), 8.38 (2H, OH, D<sub>2</sub>O exchanged) and 8.74 (2H, MeNH<sub>2</sub><sup>+</sup>, D<sub>2</sub>O exchanged) that confirmed the presence of the three hydroxyl groups at C2, C4 and C5, and that of the protonated secondary amino group on the side chain. As earlier reported, HRMS did not allow to obtain the exact mass of THMA but that of 5,6-dihydroxyindole species. Only, derivatization with methyl chloroformate provided a means of converting the highly reactive THMA to a stable derivative then avoiding the cyclization into indole (22). HRMS (ESI) *m/z* calcd for [M +

Na]<sup>+</sup> 200.06822; found, 200.06823 (5,6-dihydroxyindole species). However, it was possible to detect THMA by LC-MS (see Figure 5 below).

## Electrochemistry

Controlled-potential electrolyses were carried out in a cylindrical three-electrode divided cell (9 cm diameter), using a Voltalab 32 electrochemical analyser (Radiometer, Copenhagen). In the main compartment, a cylindrical platinum grid (area = 60 cm<sup>2</sup>) served as the anode (working electrode). A platinum sheet was placed in the concentric cathodic compartment (counter-electrode), which was separated from the main compartment with a glass frit. The reference electrode was an Ag/AgCl electrode, to which all potentials quoted are referred.

## 6-(*N*-acetylcystein-*S*-yl)-2,4,5-trihydroxymethamphetamine **5**. Procedure A

A solution of THMA, HBr (69.5 mg, 0.25 mmol), in 0.2 M HCl (250 mL), was oxidized under nitrogen at 10 °C at a platinum grid whose potential was fixed at + 1.0 V versus Ag/AgCl. After the consumption of 2 electrons per molecule, 2 equiv of *N*-acetylcysteine (83 mg, 0.50 mmol) were added to the pale orange solution, which slowly turned yellow. After 50 min, the reaction mixture was frozen at –80 °C and then freeze-dried. The residue was subdivided into fractions of about 25 mg. Each fraction was dissolved in 2 mL of water and then purified by semipreparative reversed-phase HPLC, using a mixture of solvent A/solvent B 78/22 as the eluent (flow rate: 4.5 mL min<sup>–1</sup>, detection: 292 and 264 nm). Fractions containing 6-(*N*-acetylcystein-*S*-yl)-2,4,5-trihydroxy-methamphetamine **5** were collected, immediately frozen at –80 °C, and then freeze-dried. Compound **5** (diastereomeric mixture) was isolated as a pale pink solid (64 mg, 0.18 mmol) in 71% yield. Its degree of purity (96.5%) was determined by analytical HPLC (eluent, solvent A/B 90/10; flow rate, 0.65 mL min<sup>–1</sup>). mp > 110 °C (dec.); UV absorption (0.2 M aqueous HCl) λ<sub>max</sub> = 253 (ε = 2420 mol<sup>–1</sup> L cm<sup>–1</sup>) and 307 nm (ε = 3118 mol<sup>–1</sup> L cm<sup>–1</sup>). <sup>1</sup>H NMR (D<sub>2</sub>O) δ 1.30 (d, *J* = 6.5 Hz, 3H), 1.76 (s, 3H), 2.56 (s, 3H), 3.03 (m, 3H), 3.27 (m, 1H), 3.29 (m, 1H), 4.23 (m, 1H), 6.38 (s, 1H), 6.44 (s, 1H). <sup>13</sup>C (CDCl<sub>3</sub>) Diastereoisomer A: δ 14.8, 21.4, 30.2, 31.1, 34.5, 53.2, 56.4, 105.2, 117.6, 120.3, 139.9, 143.9, 147.9, 173.8; Diastereoisomer B: δ 14.8, 21.4, 30.2, 31.2, 34.5, 53.4, 56.4, 105.2, 117.7, 120.4, 139.9, 143.9, 147.9, 173.8. Note, when the <sup>1</sup>H NMR spectra of THMA was performed in DMSO D<sub>6</sub>, four additional signals were recorded at 8.26 (1H, *NHCOMe*, D<sub>2</sub>O exchanged), 8.38 (2H, OH, D<sub>2</sub>O exchanged), 9.04 (1H, OH, D<sub>2</sub>O exchanged) and 9.42 (1H, CO<sub>2</sub>H, D<sub>2</sub>O exchanged) that confirmed the presence of the three hydroxyl groups at C2, C4 and C5, that of the acetylated amino group and that of the carboxylic acid function. As mentioned in the case of THMA, HRMS did not allow to obtain the exact mass of 6-NAC-THMA but that of its corresponding 5,6-dihydroxyindole species. HRMS (ESI) *m/z* calcd for [M + Na]<sup>+</sup> 361.08282; found, 361.08286.

For biological evaluation, a second purification was performed by semipreparative reversed-phase HPLC, using a mixture of solvent A/solvent B 92/8 as the eluent (flow rate: 10.5 mL min<sup>–1</sup>). Then, compound **5** could be isolated with 99.5% purity grade (see the supporting information).

## Procedure B

A solution of THMA, HBr **4** (69.5 mg, 0.25 mmol) in 10<sup>–2</sup> M sodium phosphate buffer (250 mL, pH 7.4) containing 5 equiv of *N*-acetylcysteine (208 mg, 1.25 mmol) was oxidized under nitrogen at 10 °C at a platinum grid whose potential was fixed at + 0.4 V versus Ag/AgCl. After the consumption of 1.75 electron per molecule, the resulting red solution was acidified to pH 2.0 with 0.2 M HCl. The resulting solution was frozen at –80 °C and then freeze-dried. Semipreparative reversed-phase HPLC was performed using the following mobile phase gradient (flow rate: 5.0 mL min<sup>–1</sup>): 0–10 min, mixture of solvent A/solvent B

80/20; 10–70 min, mixture of solvent A/solvent B from 80/20 to 100% solvent B. Fractions containing 6-(*N*-acetylcystein-*S*-yl)-2,4,5-trihydroxymethamphetamine **5** were collected, immediately frozen at  $-80^{\circ}\text{C}$ , and then freeze-dried. Compound **5** was isolated in 27% yield (24.0 mg, 0.07 mmol). 21% of the starting THMA (10.5 mg, 0.05 mmol) were also recovered because the electrolysis was stopped before the end of the oxidation (after the consumption of 1.75 electron per molecule) since, in pH 7.4 buffer, compound **5** underwent oxidative cyclization into an indole species which rapidly polymerized as do other indoles of this nature (29).

### Enzymatic oxidation

Mushroom tyrosinase (12500 units) was added to a solution of THMA, HBr **4** (69.5 mg, 0.25 mmol) containing 5 equiv of *N*-acetylcysteine (208 mg, 1.25 mmol) in  $10^{-2}$  M sodium phosphate buffer (250 mL, pH 7.4) at  $37^{\circ}\text{C}$ . The solution became immediately red. After 10 min of reaction at  $37^{\circ}\text{C}$ , the solution was acidified to pH 2.0 with concentrated HCl, frozen at  $-80^{\circ}\text{C}$  and then freeze-dried. Semipreparative reversed-phase HPLC was performed using the following mobile phase gradient (flow rate:  $5.0\text{ mL min}^{-1}$ ): 0–10 min, mixture of solvent A/solvent B 80/20; 10–80 min, mixture of solvent A/solvent B from 80/20 to 100% solvent B. Fractions containing 6-(*N*-acetylcystein-*S*-yl)-2,4,5-trihydroxymethamphetamine **5** were collected, immediately frozen at  $-80^{\circ}\text{C}$ , and then freeze-dried. Compound **5** was isolated in 21.5% yield (19.2 mg, 0.05 mmol). Note 14.5% of THMA (7.5 mg, 0.04 mmol) were also recovered.

### Biological Studies

Male albino Sprague-Dawley rats weighing approximately 300 grams were used. Animals were housed in a colony room maintained at  $22 \pm 2^{\circ}\text{C}$  with free access to food and water. Lighting in the room was automatically regulated on a 12:12 h light: dark cycle. Animals were single housed throughout. The facilities used are accredited by the American Association for the Assessment and Accreditation of Laboratory Animal Care. All experimental procedures were approved by the Institutional Animal Care and Use Committee at the Johns Hopkins University School of Medicine and were in accordance with the National Institutes of Health Guide for the Care and Use of Laboratory Animals Housing.

To evaluate of the lasting effects of THMA and 6-NAC-THMA on brain 5-HT axonal markers, five experiments were performed. The purpose and design of each of these experiments were as follows:

Experiment 1 assessed regional brain 5-HT and 5-HIAA levels one week after administration of newly synthesized THMA. THMA, as the hydrobromide salt, was administered into the right lateral ventricle of rats at two different doses (250 and 1000 nmol). Doses refer to the base form. These doses were selected on the basis of previous studies (23, 24). Rats received either 10  $\mu\text{L}$  of artificial cerebrospinal fluid (aCSF) (control group,  $N = 5$ ), 250 nmol of THMA ( $N = 6$ ), or 1000 nmol of THMA ( $N = 7$ ).

Experiment 2 determined if the lasting effect of THMA on central 5-HT neuronal markers could be blocked with a 5-HT transporter blocker, fluoxetine. There were four treatment groups ( $n=5-7$  per group): 1) SAL/aCSF; 2) Fluox/aCSF; 3) SAL/THMA, 4) Fluox/THMA. Rats received saline or fluoxetine (10 mg/kg, i.p.) 65 and 5 min prior to injection of THMA (150  $\mu\text{g}$ ) into the lateral ventricle. THMA was dissolved in aCSF immediately prior to intraventricular injection. One week after treatment, rats were sacrificed for determination of brain 5-HT and 5-HIAA levels.

Experiment 3 tested for the presence of THMA in the brain of animals treated with a high neurotoxic dose of MDMA (80 mg/kg; s.c.). Six rats were treated with MDMA: 3 were examined 1.5 h after MDMA administration; the other 3 were examined 3 hours after MDMA administration. Cortical and hippocampal tissue from these animals was analyzed for THMA, MDMA and various MDMA metabolites, as below. These times for analysis were selected on the basis of prior pharmacokinetic studies of MDMA in the rat indicating that these times correspond to peak concentrations of MDMA [i.e. times when maximum concentrations of precursor would be available for potential conversion into THMA (20)]. Also, after intracerebroventricular administration, the highest levels of THMA were evident 30 to 120 minutes later (see Figure 6).

Experiment 4 determined if THMA, an inherently unstable molecule, could be reliably measured in brain tissue after central doses that produce a lasting effect on brain 5-HT and 5-HIAA, namely 250 and 1000 nmol (see Figure 2). THMA (250 or 1000 nmol) was infused into the right lateral ventricle of rats (N = 12 for each dose). Animals were then divided into subgroups (N = 3 at each time point) and sacrificed at various time points (0.5, 1, 2, and 4 h) after treatment. Regional brain levels of THMA were measured, as below.

Experiment 5 assessed regional brain 5-HT and 5-HIAA levels two weeks after administration of 6-NAC-THMA, the thioether conjugate of THMA. 6-NAC-THMA was administered directly into the right frontal cortex. Rats received either 1  $\mu$ L of aCSF (control group, N = 6) or 42 nmol of 6-NAC-THMA (N = 8), or 52 nmol of 5,7-dihydroxytryptamine (5,7-DHT) (positive control group, N = 6, single dose). Animals treated with aCSF and 6-NAC-THMA received four consecutive doses, with each dose administered 12 h apart. The neurotoxin 5,7-DHT was administered in a single dose. Dose and frequency chosen are the same that were used in previous studies to test for the neurotoxic potential of various thioether conjugates derived from HHMA and/or HHA (15, 16, 18, 20).

### **Intracerebroventricular administration**

Animals were anesthetized with a sodium pentobarbital (60 mg/kg, i.p.) and the head was shaved and placed into a stereotaxic apparatus. Using a surgical scalpel, a mid-sagittal incision was made to expose the skull. A small burr hole was made with a hand drill: (–) 0.92 mm from bregma, (–) 1.4 mm lateral to the midline. A 10  $\mu$ L Hamilton 7000 series glass syringe (Hamilton Co., Reno, NV) containing the various injection solutions was inserted (–) 3.5 mm dorsoventrally (35). Artificial CSF serving as a vehicle control was prepared as described previously by Miller et al. (15). Ten microliter of the drug solution was injected manually into the right ventricle at a rate of 10  $\mu$ L over 2 min. After the injection was completed, the needle was left in the ventricle for an additional 2 min.

### **Intracortical administration**

Animals were anesthetized with xylazine (25 mg/kg, i.p.) and ketamine (35 mg/kg i.p.). Guide cannulae (20 gauge; Plastic One, Roanoke, VA) were surgically implanted into the right frontal cortex [anteroanterior, 3.0 mm; mediolateral, 2.0 mm; dorsoventral, 2.0 mm (35)]. Cannulae were fixed to the skull with dental acrylic (Ortho-Jet, Lang Dental, Wheeling, IL) and two stainless steel screws. Dummy cannulae were placed in the guide cannulae, and animals were individually housed and allowed a 7-day recovery period. The dummy cannulae were replaced with internal cannulae (24 gauge; Plastic One) connected to PE 20 tubing that in turn was connected to a 1  $\mu$ L Hamilton 7000 series glass syringe (Hamilton Co., Reno, NV) containing the various injection solutions. Artificial CSF served as a vehicle control and was prepared as described previously by Miller et al. (20). One microliter of the drug solution was injected manually into the frontal cortex at a rate of 0.2  $\mu$ L over 5 min for a total of four consecutive doses, with each dose administered 12 h apart.



After the injection was completed, the internal cannulae were left in the cortex for an additional 2 min. Animals were awake but gently restrained during the injections. After injection, the dummy cannulae were replaced.

### Brain Dissection

Rats were killed by decapitation and the striatum, hippocampus and cerebral cortex were dissected free as previously described (36). Immediately after dissection, tissue parts were wrapped in aluminum foil and stored in liquid nitrogen until assay.

### Regional brain 5-HT and 5-HIAA determination

Tissue samples were analyzed for their content of 5-HT and 5-HIAA 1 or 2 weeks after drug treatment by means of high performance liquid chromatography coupled with electrochemical detection (HPLC-EC) as previously described (7).

### Determination of brain THMA and MDMA metabolite concentrations

For determination of brain concentrations of THMA, samples were prepared and analyzed using LC-MS methods. In particular, aliquots of rat cortex (approximately 100 mg) and hippocampus (approximately 50 mg) were weighed and for each microgram of tissue, 10  $\mu$ L of internal standard solution (pholedrine) was added. After homogenization in 0.01 M HCl (preserved with 6 % of each 250 mmol SMBS and 250 mmol EDTA) with a Polytron homogenization unit (model PT 10–35, 15 s, setting 6; Kinematica Inc., Bohemia, NY), the samples were centrifuged (16,000g for 10 min), and the supernatant was transferred to autosampler vials. Aliquots (5 $\mu$ L) were injected into the LC-MS system. All samples were analyzed using an Agilent Technologies (AT, Waldbronn, Germany) AT Series 1100 LC/MSD, VL version, using electrospray ionization (ESI) in positive ionization mode, including an AT 1100 Series HPLC system which consisted of a degasser, a quaternary pump, a column thermostat, and an autosampler. Isocratic elution was performed on a Zorbax 300-SCX column (Narrow-Bore 2.1  $\times$  150 mm, 5  $\mu$ m) and a Zorbax SCX guard column (4.6  $\times$  12.5 mm, 5  $\mu$ m). The mobile phase consisted of 5 mM aqueous ammonium formate adjusted to pH 3 with formic acid (eluent A) and acetonitrile (eluent B). Samples were analyzed in positive (selected ion monitoring) SIM mode with the following ions:  $m/z$  198 (target ion), 167 for THMA,  $m/z$  196 (t), 165 for the cyclic indoline form of THMA, and  $m/z$  166 (t), 135 for pholedrine (IS). Fragmentor voltage, 100 V. The linear range was 5 to 100  $\mu$ g/g for THMA as well as for the indoline species. The lowest point of the calibration curve was defined as the limits of quantitation of the method (5 $\mu$ g/g). For determination of MDMA and its metabolites HHMA, HMMA, and MDA, samples were prepared and analyzed using previously described LC-MS methods (37).

### Statistics

The significance of differences between means was determined using one-way analysis of variance (ANOVA) followed by Tukey's multiple comparison test. Statistical analyses were performed using Prism, Version 3.02 (GraphPad Software, Inc. San Diego, CA, USA). Differences were considered significant if  $p < 0.05$ .

## Results and Discussion

### Synthesis of THMA

THMA was synthesized in a straightforward manner (Scheme 2), starting from commercially available 2,4,5-trimethoxybenzaldehyde. Briefly, the previously reported Knoevenagel condensation between 2,4,5-trimethoxybenzaldehyde and nitroethane (34) quantitatively led to  $\beta$ -methyl- $\beta$ -nitrostyrene **1**, which was converted, after reduction of the

nitro group and hydrolysis of the imine function, into the corresponding 2,4,5-trimethoxyphenylacetone **2** in 80.5% yield. Then, acid-catalyzed reductive amination by sodium triacetoxyborohydride (**38**) quantitatively yielded 2,4,5-trimethoxymethamphetamine **3**. Finally, complete demethylation of **3** using hydrobromic acid heated at reflux, afforded THMA **4** in 76% yield. Interestingly, this four step reaction sequence produced THMA in a markedly improved overall yield (60%) when compared with that of the previously described procedure, starting from commercially available 3,4-(methylenedioxy)phenol, for which the overall yield did not exceed 5% after seven steps (24). Although it was previously reported that THMA could be synthesized from 2,4,5-trimethoxybenzaldehyde by modification of the procedure for 4-hydroxy-3-methoxymethamphetamine, no details of the experiments were provided (22). So, the experiments and the spectroscopic characterizations are thoroughly detailed in this work.

### Electrosynthesis of 6-NAC-THMA **5**

As previously described in the case of 6-hydroxydopamine (**39**), 2,4,5-trihydroxymethamphetamine was poorly stable in potassium phosphate buffer (pH 7.4) and rapidly air oxidized to a putative *p*-quinone species. At pH 7.4, the ionization of the phenol group at the 4 position [ $pK_a = 4-5$ , as reported for 6-OHDA (**39**)] facilitated the deprotonation of the secondary amine function at the origin of the intramolecular cyclization, leading to an indoline intermediate. This was converted into a redox active 5,6-dihydroxyindole species which, after subsequent oxidation reaction, afforded insoluble melanin-like polymers (Scheme 3, path a). To overcome this problem, we decided to adapt our electrochemical procedure, previously described for the preparation of thioether conjugates of HHMA (**40**, **41**), to the synthesis of 6-NAC-THMA **5**. So, the anodic oxidation of THMA **4** was conducted under acidic conditions (Scheme 3, path b), in the absence of *N*-acetylcysteine (NAC) because 6-NAC-THMA **5** was also electroactive at the applied potential, giving no desired additional oxidation products.

Controlled potential electrolysis was used as a preparative method for the isolation of 6-NAC-THMA **5**. When the controlled potential of the platinum anode was fixed at + 1.0 V versus Ag/AgCl, which is at a potential for which THMA could be oxidized to the *p*-quinone species, a coulometric value of  $2.0 \pm 0.1$  was found for the number of electrons involved in the oxidation of one molecule of THMA into the transient *p*-quinone species. The latter was rather stable in aqueous 0.2 M HCl as shown by monitoring the UV absorption spectrum in the course of the electrolysis (Figure 1). After the application of the potential, a decrease in the UV absorption band shown by THMA at 292 nm ( $\epsilon = 4300 \text{ mol}^{-1} \text{ L cm}^{-1}$ ) was observed, while two new bands at 264 and 389 nm developed. Spectral changes showed three isosbestic points at 230, 283 and 309 nm, indicating that a simple equilibrium between two species was shifted (Figure 1, spectra a-e). Subsequent addition of 2 equiv of *N*-acetylcysteine resulted in the slow discoloration of the pale orange solution due to the formation of the catechol-thioether conjugate **5**, which was identified by the change in the UV absorption spectrum (Figure 1, spectra e-i), showing new absorption maxima at 261 and 298 nm. Treatment of the electrolysis solution afforded, after semipreparative reversed-phase HPLC (See Experimental Section), 6-NAC-THMA **5** in 71% yield.

In a second experiment aimed at comparing the results of anodic oxidation with that of enzymatic procedure reported below, the electrolysis was performed in potassium phosphate buffer (pH 7.4), in the presence of NAC, in other words, under the experimental conditions required for enzymatic oxidation. After the application of the potential, the electrolysis solution rapidly became red, in agreement with the formation of quinonoid species. This was substantiated by monitoring the UV absorption spectrum in the course of the electrolysis. A decrease in the UV absorption band at 292 nm was recorded while new bands at 278 and 489 nm developed. Contrary to what has been observed under acidic conditions, spectral

changes did not show isosbestic points. Consequently, to limit the decomposition of the electrogenerated catechol-thioether conjugate **5** which was electroactive at the applied potential, the electrolysis was stopped after the consumption of 1.75 electron per molecule. Treatment of the electrolysis solution afforded, after semipreparative reversed-phase HPLC, 6-NAC-THMA **5** in 27% yield.

### Enzymatic procedure for the synthesis of 6-NAC-THMA **5**

To ensure that 6-NAC-THMA **5** could be formed enzymatically, THMA was oxidized with mushroom tyrosinase in the presence of 5 equiv of NAC (See Experimental Section), a method previously reported for the synthesis of thioether conjugates of HHMA (18, 25, 42). Because of the rapid degradation of the solution at 37°C, the reaction was stopped after only 10 min by acidification of the reaction mixture to pH 2.0 with concentrated HCl. After semipreparative reversed-phase HPLC, 6-NAC-THMA **5** was isolated in 21% yield. Although 6-NAC-THMA **5** can be prepared enzymatically, this procedure was not adapted for routine synthesis because it was too expensive and not suitable for yielding substantial amounts of thioether conjugates. In this respect, the electrosynthesis performed under acidic conditions proved to be particularly attractive for routine synthesis, leading to 6-NAC-THMA **5** in high yield (71%).

### Biological studies of THMA **4**

THMA **4** administered into the right lateral ventricle of rats produced a significant lasting depletion of 5-HT and 5-HIAA in the cortex and hippocampus (Figure 2). 5-HT and 5-HIAA levels were also reduced in the striatum but the reductions did not achieve statistical significance. In contrast, significant effects on DA were evident in the striatum (Figure 3). Taken together, these results confirm previous reports that THMA has the potential to produce lasting effects on brain 5-HT and DA neurons (23, 24).

The lasting effect of THMA on brain 5-HT neurons could be blocked with the 5-HT uptake inhibitor fluoxetine (Figure 4). This observation indicates that the lasting effect of THMA on brain 5-HT neurons, like that of MDMA, is dependent on intact 5-HT transporter function (30, 43). Further, it suggests that THMA could play a role in MDMA's long-term effects on brain 5-HT neurons.

If THMA is, in fact, the metabolite that mediates MDMA neurotoxicity, its presence in brain would be anticipated. We therefore sought to identify THMA in the brain of MDMA-treated animals. While other *O*-demethylenated MDMA metabolites of MDMA (HHMA and HMMA) could be readily and reliably detected in the brain of rats treated with a high neurotoxic dose of MDMA (80 mg/kg), THMA could not be detected in either the cortex or hippocampus, at either 1.5 or 3 hours after MDMA administration (Figure 5).

Recognizing that our inability to detect THMA in the brain of MDMA-treated rats might be due to the inherent instability of the THMA molecule, we next carried out studies to determine the stability of THMA *in vivo*. In particular, we administered THMA to rats intracerebroventricularly, then attempted to measure THMA in various rat brain regions at several times after THMA administration. Figure 6 shows time-concentration profiles of THMA in the cortex, hippocampus and striatum of rats treated identically as those whose lasting 5-HT and 5-HIAA depletions are shown in Figure 2. THMA levels peaked approximately 0.5–1 h after THMA administration and could be measured up to 4 hours. These results demonstrate that it is feasible to detect and reliably measure THMA (and its indoline formed *via* cyclization – not shown) in rat brain tissue for several hours after its intracerebroventricular administration. Thus, it appears that our inability to identify THMA in the rat brain after peripheral MDMA administration is not related to instability of the

THMA molecule. The absence of detectable levels of THMA after MDMA administration casts doubt on the view that THMA, at least in its free (unconjugated) form, mediates MDMA's lasting effects on brain 5-HT neurons. At this time, it cannot be stated with absolute certainty that other conjugated forms of THMA, such a sulfate or glucuronic conjugates, are not present in brains of MDMA-treated rats because the present THMA analyses were done without performing conjugate cleavage (because the cleavage procedure results in THMA degradation and disappearance).

Notably, inspection of Figures 2 and 6 shows that there was no correlation between THMA concentrations and lasting 5-HT deficits in various rat brain regions. That is, higher concentrations of THMA were not associated with greater 5-HT deficits. This may be yet another indication that THMA does not mediate the long-term effects of MDMA on brain 5-HT neurons because, in general, there is an excellent correlation between brain MDMA concentrations and lasting 5-HT deficits (20). In considering the lack of correlation between THMA concentrations and regional brain 5-HT deficits, it is also important to take into account that 5-HT terminals in different brain regions may differ in their susceptibility to various neurotoxicants, including THMA. Further, it is possible that 5-HT terminals in the striatum are less affected because some THMA in this brain region may be sequestered within DA terminals, effectively reducing the amount of THMA to which 5-HT terminals are exposed.

### Biological studies of 6-NAC-THMA 5

Given reports implicating thioether conjugates of *O*-demethylated metabolites of MDMA as mediators of MDMA neurotoxicity (10, 15–18, 27, 28, but see 20), we next assessed the neurotoxic potential of 6-NAC-THMA 5, a thioether conjugate of THMA. These studies involved direct injection of 6-NAC-THMA 5 into cortical tissue, using the known 5-HT neurotoxin, 5,7-DHT, as a positive control. As expected, 5,7-DHT produced lasting depletions of both 5-HT and 5-HIAA in brain (Figure 7). In contrast, 6-NAC-THMA 5 was without long-term effects on brain 5-HT neuronal markers. These results suggest that 6-NAC-THMA 5 lacks significant 5-HT neurotoxic potential, and do not support the view that this particular thioether conjugate of THMA is responsible for mediating MDMA-induced 5-HT neurotoxicity.

### Conclusions

THMA produces lasting effects on brain 5-HT neurons. The lasting effect of THMA on brain 5-HT neurons, like that of MDMA, is dependent upon intact 5-HT transporter function. In contrast to other *O*-demethylated MDMA metabolites (HHMA, HMMA), THMA was not detected in brain tissue of rats treated peripherally with a high neurotoxic dose of MDMA. Inability to detect THMA in the brain after peripheral MDMA administration was not due to instability of the THMA molecule, because exogenous THMA administered centrally could be readily detected in rat brain for several hours after intracerebroventricular administration. The thioether conjugate of THMA, 6-NAC-THMA, lacks 5-HT neurotoxic potential, as evidenced by the fact that it fails to produce lasting effects on brain 5-HT axonal markers. Taken together, these observations suggest that neither THMA 4 nor 6-NAC-THMA 5 is directly responsible for MDMA neurotoxicity but leave open the possibility that forms of THMA different than those measured here (e.g., different THMA conjugates or oxidized cyclic forms) could be involved. Additional research is required to test these possibilities.

### Supplementary Material

Refer to Web version on PubMed Central for supplementary material.

## Acknowledgments

### Funding Sources

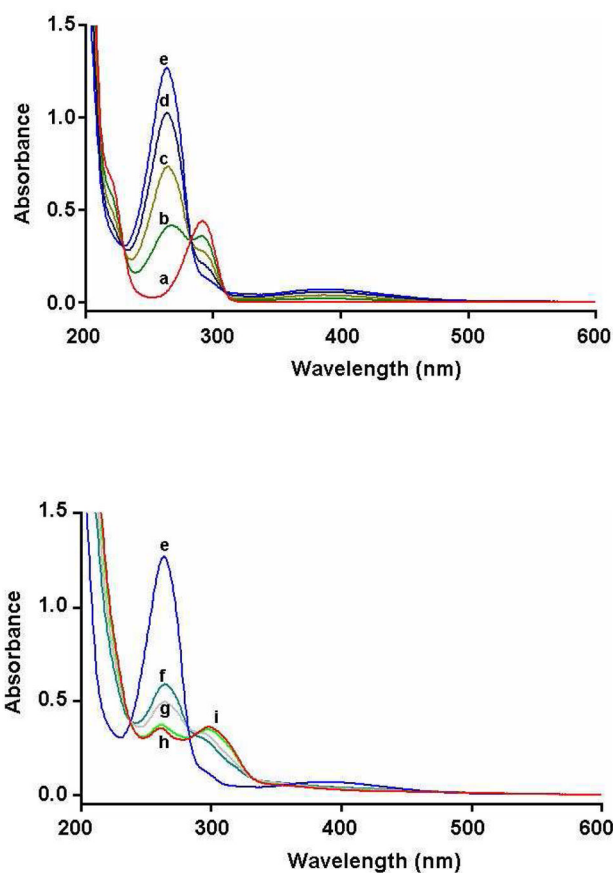
C.M.M. is a PhD student funded by the French MENRT. This Research was supported by the joint grants of the « Mission Interministérielle de Lutte contre la Drogue et la Toxicomanie » (MILDT) and the « Institut National de la Santé et de la Recherche Médicale » (INSERM). (Appel à projets commun 2007 MILDT-INSERM « Recherche sur les drogues et la toxicomanie ») (to M.L.) as well as by NIH grants DA 05707 and DA 01796401 (to G.A.R.).

## References

1. Green AR, Mehan AO, Elliott JM, O'Shea E, Colado MI. The pharmacology and clinical pharmacology of 3,4-methylenedioxymethamphetamine (MDMA, "ecstasy"). *Pharmacol Rev.* 2003; 55:463–508. [PubMed: 12869661]
2. Sakar S, Schmued L. Neurotoxicity of ecstasy (MDMA): an overview. *Curr Pharm Biotechnol.* 2010; 11:460–469. [PubMed: 20420572]
3. Molliver ME, Berger UV, Mamounas LA, Molliver DC, O'Hearn E, Wilson MA. Neurotoxicity of MDMA and related compounds: anatomic studies. *Ann N Y Acad Sci.* 1990; 600:649–661. [PubMed: 1979216]
4. Commins DL, Vosmer G, Virus RM, Woolverton WL, Schuster CR, Seiden LS. Biochemical and histological evidence that methylenedioxymethylamphetamine (MDMA) is toxic to neurons in the rat brain. *J Pharmacol Exp Ther.* 1987; 241:338–345. [PubMed: 2883295]
5. Callahan BT, Cord BJ, Ricaurte GA. Long-term impairment of anterograde axonal transport along fiber projections originating in the rostral raphe nuclei after treatment with fenfluramine or methylenedioxymethamphetamine. *Synapse.* 2001; 40:113–121. [PubMed: 11252022]
6. Yamamoto BK, Moszczynska A, Gudelsky GA. Amphetamine toxicities: classical and emerging mechanisms. *Ann N Y Acad Sci.* 2010; 1187:101–121. [PubMed: 20201848]
7. Mehan A, Yuan J, Hatzidimitriou G, Irvine RJ, McCann UD, Ricaurte GA. Pharmacokinetic profile of single and repeated oral doses of MDMA in squirrel monkeys: relationship to lasting effects on brain serotonin neurons. *Neuropsychopharmacology.* 2006; 31:339–350. [PubMed: 15999148]
8. Easton N, Marsden CA. Ecstasy: are animal data consistent between species and can they translate to humans? *J Psychopharmacol.* 2006; 20:194–210. [PubMed: 16510478]
9. Schmidt CJ, Wu L, Lovenberg W. Methylenedioxymethamphetamine: a potentially neurotoxic amphetamine analogue. *Eur J Pharmacol.* 1986; 124:175–178. [PubMed: 2424776]
10. Capela JP, Carmo H, Remiao F, Lourdes Bastos M, Meisel A, Carvalho F. Molecular and cellular mechanisms of ecstasy-induced neurotoxicity: an overview. *Mol Neurobiol.* 2009; 39:210–271. [PubMed: 19373443]
11. Schmidt CJ, Taylor VL. Direct central effects of acute methylenedioxy-methamphetamine on serotonergic neurons. *Eur J Pharmacol.* 1988; 156:121–131. [PubMed: 2463176]
12. Paris JM, Cunningham KA. Lack of serotonin neurotoxicity after intraraphe microinjection of ( $\pm$ )-3,4-methylenedioxymethamphetamine (MDMA). *Brain Res Bull.* 1992; 28:115–119. [PubMed: 1347247]
13. Esteban B, O'Shea E, Camarero J, Sanchez V, Green AR, Colado MI. 3,4-Methylenedioxymethamphetamine induces monoamine release, but not toxicity, when administered centrally at a concentration occurring following a peripherally injected neurotoxic dose. *Psychopharmacology (Berl).* 2001; 154:251–260. [PubMed: 11351932]
14. Escobedo I, O'Shea E, Orio L, Sanchez V, Segura M, de la Torre R, Farre M, Green AR, Colado MI. A comparative study on the acute and long-term effects of MDMA and 3,4-dihydroxymethamphetamine (HHMA) on brain monoamine levels after i. p or striatal administration in mice. *Br J Pharmacol.* 2005; 144:231–241. [PubMed: 15665862]
15. Miller RT, Lau SS, Monks TJ. 2,5-Bis-(glutathion-S-yl)-alpha-methyl-dopamine, a putative metabolite of ( $\pm$ )-3,4-methylenedioxyamphetamine, decreases brain serotonin concentrations. *Eur J Pharmacol.* 1997; 323:173–180. [PubMed: 9128836]

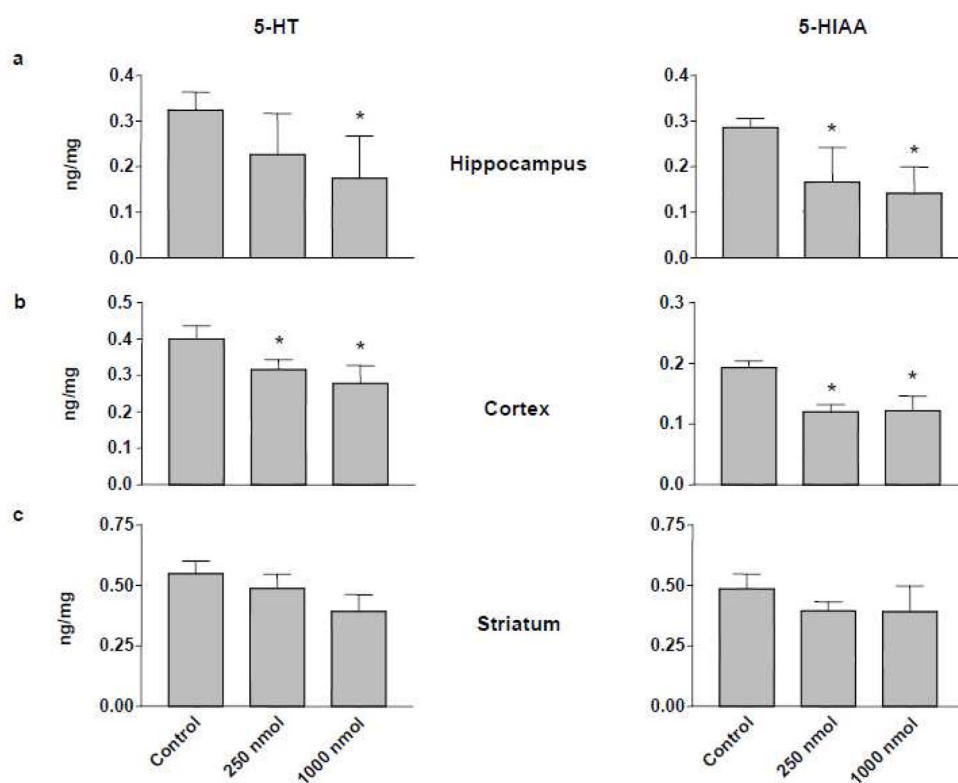
16. Bai F, Lau SS, Monks TJ. Glutathione and N-acetylcysteine conjugates of  $\alpha$ -methyl dopamine produce serotonergic neurotoxicity: possible role in methylenedioxyamphetamine-mediated neurotoxicity. *Chem Res Toxicol.* 1999; 12:1150–1157. [PubMed: 10604863]
17. Monks TJ, Jones DC, Bai F, Lau SS. The role of metabolism in 3,4-(+)-methylenedioxyamphetamine and 3,4-(+)-methylenedioxymethamphetamine (ecstasy) toxicity. *Ther Drug Monit.* 2004; 26:132–136. [PubMed: 15228153]
18. Jones DC, Duvauchelle C, Ikegami A, Olsen CM, Lau SS, de la Torre R, Monks TJ. Serotonergic neurotoxic metabolites of ecstasy identified in rat brain. *J Pharmacol Exp Ther.* 2005; 313:422–431. [PubMed: 15634943]
19. Steele TD, Brewster WK, Johnson MP, Nichols DE, Yim GK. Assessment of the role of alpha-methylepine in the neurotoxicity of MDMA. *Pharmacol Biochem Behav.* 1991; 38:345–351. [PubMed: 1676172]
20. Mueller M, Yuan J, Felim A, Neudörffer A, Peters FT, Maurer HH, McCann UD, LARGERON M, Ricaurte GA. Further studies on the role of metabolites in ( $\pm$ )-3,4-methylenedioxymethamphetamine-induced serotonergic neurotoxicity. *Drug Metab Dispos.* 2009; 37:2079–2086. [PubMed: 19628751]
21. McCann UD, Ricaurte GA. Major metabolites of ( $\pm$ )-3,4-methylenedioxyamphetamine (MDA) do not mediate its toxic effects on brain serotonin neurons. *Brain Res.* 1991; 545:279–282. [PubMed: 1860050]
22. Lim HK, Foltz RL. Ion trap tandem mass spectrometric evidence for the metabolism of 3,4-(methylenedioxy)methamphetamine to the potent neurotoxins 2,4,5-trihydroxymethamphetamine and 2,4,5-trihydroxyamphetamine. *Chem Res Toxicol.* 1991; 4:626–632. [PubMed: 1687259]
23. Zhao Z, Castagnoli N, Ricaurte GA, Steele T, Martello M. Synthesis and neurotoxicological evaluation of putative metabolites of the serotonergic neurotoxin 2-(methylamino)-1-[3,4-(methylenedioxy)phenyl]propane[(Methylenedioxy)methamphetamine]. *Chem Res Toxicol.* 1992; 5:89–94. [PubMed: 1349835]
24. Johnson M, Elayan I, Hanson GR, Foltz RL, Gibb JW, Lim HK. Effects of 3,4-dihydroxymethamphetamine and 2,4,5-trihydroxymethamphetamine, two metabolites of 3,4-methylenedioxymethamphetamine, on central serotonergic and dopaminergic systems. *J Pharmacol Exp Ther.* 1992; 261:447453.3.
25. Erives GV, Lau SS, Monks TJ. Accumulation of neurotoxic thioether metabolites of 3,4-( $\pm$ )-methylenedioxymethamphetamine in rat brain. *J Pharmacol Exp Ther.* 2008; 324:284–291. [PubMed: 17906065]
26. Pizarro N, de la Torre R, Joglar J, Okumura N, Perfetti X, Lau SS, Monks TJ. Serotonergic neurotoxic thioether metabolites of 3,4-methylenedioxymethamphetamine (MDMA, « ecstasy »): synthesis, isolation and characterization of diastereoisomers. *Chem Res Toxicol.* 2008; 21:2272–2279. [PubMed: 19548351]
27. Perfetti X, O’Mathuna B, Pizarro N, Cuyas E, Khymenets O, Almeida B, Pellegrini M, Pichini S, Lau SS, Monks TJ, Farré M, Pascual A, Joglar J, de La Torre R. Neurotoxic thioether adducts of MDMA identified in human urine after ecstasy ingestion. *Drug Metab Dispos.* 2009; 37:1448–1455. [PubMed: 19349378]
28. Capela JP, Macedo C, Branco PS, Ferreira LM, Lobo AM, Fernandes E, Remiao F, Bastos ML, Dirnagl U, Meisel A, Carvalho F. Neurotoxicity mechanisms of thioether ecstasy metabolites. *Neuroscience.* 2007; 146:1743–1757. [PubMed: 17467183]
29. Liang Y-O, Plotsky PM, Adams RN. Isolation and identification of an in vivo reaction product of 6-hydroxydopamine. *J Med Chem.* 1977; 20:581–583. [PubMed: 850243]
30. Schmidt CJ. Neurotoxicity of the psychedelic amphetamine, methylenedioxymethamphetamine. *J Pharmacol Exp Ther.* 1987; 240:1–7. [PubMed: 2433425]
31. Borgman RJ, Baylor MR, McPhillips JJ, Stitzel RE.  $\alpha$ -Methyl dopamine derivatives. Synthesis and pharmacology. *J Med Chem.* 1974; 17:427–430. [PubMed: 4830540]
32. Morgan PH, Beckett AH. Synthesis of some N-oxygenated products of 3,4-dimethoxyamphetamine and its N-alkyl derivatives. *Tetrahedron.* 1975; 31:2595–2601.
33. Cannon JG, Perez Z, Long JP, Rusterholtz DB, Flynn JR, Costall B, Fortune DH, Naylor RJ. N-alkyl derivatives of ( $\pm$ )- $\alpha$ -methyl dopamine. *J Med Chem.* 1979; 22:901–907. [PubMed: 573798]

34. Milhazes N, Cunha-Oliveira T, Martins P, Garrido J, Oliveira C, Rego AC, Borges F. Synthesis and cytotoxicity profile of 3,4-methylenedioxyamphetamine (“ecstasy”) and its metabolites on undifferentiated PC12 cells: a putative structure-toxicity relation ship. *Chem Res Toxicol.* 2006; 19:1294–1304. [PubMed: 17040098]
35. Paxinos, G.; Watson, C. *The Brain in Stereotaxic Coordinates.* Academic Press, Inc; New York: 1986.
36. Heffner TG, Hartman JA, Seiden LS. A rapid method for the regional dissection of the rat brain. *Pharmacol Biochem Behav.* 1980; 13:453–456. [PubMed: 7422701]
37. Mueller M, Peters FT, Ricaurte GA, Maurer HH. Liquid chromatographic-electrospray ionization mass spectrometric assay for simultaneous determination of 3,4-methylenedioxyamphetamine and its metabolites 3,4-methylenedioxyamphetamine, 3,4-dihydroxymethamphetamine, and 4-hydroxy-3-methoxymethamphetamine in rat brain. *J Chromatogr B Analyt Technol Biomed Life Sci.* 2008; 874:1199–124.
38. Jozwiak K, Yiu-Ho Woo A, Tanger MJ, Toll L, Jimenez L, Kozocas JA, Plazinska A, Xiao RP, Wainer IW. Comparative molecular field analysis of fenoterol derivatives: a platform towards highly selective and effective  $\beta_2$ -adrenergic receptor agonists. *Bioorg Med Chem.* 2010; 18:728–736. [PubMed: 20036561]
39. Blank CL, Kissinger PT, Adams RN. 5,6-dihydroxyindole formation from oxidized 6-hydroxydopamine. *Eur J Pharmacol.* 1972; 19:391–394. [PubMed: 4640864]
40. Felim A, Urios A, Neudörffer A, Herrera G, Blanco M, Llargeron M. Bacterial plate assays and electrochemical methods: an efficient tandem for evaluating the ability of catechol-thioether metabolites of MDMA (“ecstasy”) to induce toxic effects through redox-cycling. *Chem Res Toxicol.* 2007; 20:685–693. [PubMed: 17355154]
41. Felim A, Neudörffer A, Monnet FP, Llargeron M. Environmentally friendly expeditious one-pot electrochemical synthesis of bis-catechol-thioether metabolites of ecstasy: in vitro neurotoxic effects in the rat hippocampus. *Int J Electrochem Sci.* 2008; 3:266–281.
42. Macedo C, Branco PS, Ferreira LM, Lobo AM, Capela JP, Fernandes E, de Lourdes Bastos M, Carvalho F. Synthesis and cyclic voltammetry studies of 3,4-methylenedioxyamphetamine (MDMA) human metabolites. *J Health Sci.* 2007; 53:31–42.
43. Sanchez V, Camarero J, Esteban B, Peter MJ, Green AR, Colado MI. The mechanisms involved in the long-lasting neuroprotective effect of fluoxetine against MDMA (“ecstasy”)-induced degeneration of 5-HT nerve endings in rat brain. *Br J Pharmacol.* 2001; 134:46–57. [PubMed: 11522596]

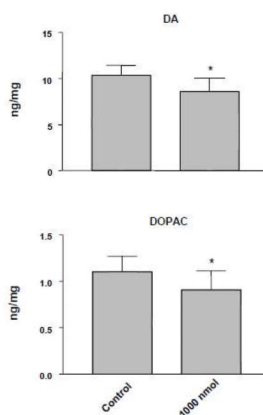


**Figure 1.** Spectrophotometric changes accompanying the electrosynthesis of 6-NAC-THMA **5**. (spectra a-e): electrochemical oxidation of THMA(1 mM), at a platinum anode ( $E = + 1.0$  V versus Ag/AgCl), in deaerated 0.2 M HCl aqueous solution: (a) 0 (before electrolysis), (b) 0.5, (c) 1.0, (d) 1.5, (e) 2.0 mol of electrons. (spectra f-i): evolution after addition of 2 equiv of *N*-acetylcysteine to the two electrons-oxidized solution: (f) 10 min after addition, (g) 20 min, (h), 40 min, (i) 50 min (end of the process). Cell thickness is 0.1 cm.

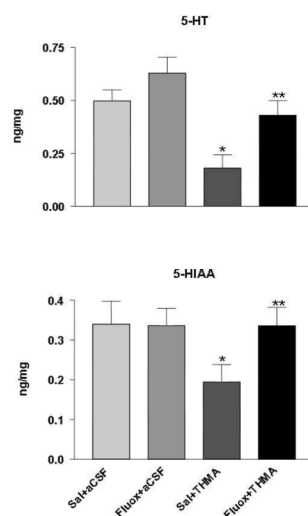




**Figure 2.** 5-HT (left panels) and 5-HIAA levels (right panels) in hippocampus (a), cerebral cortex (b), and striatum (c) of rats one week after intracerebroventricular administration of 250 or 1000 nmol THMA. Control animals received unilateral intracerebroventricular injections of an equivalent volume of aCSF. Values represent the mean  $\pm$ SD (N=5–7) side ipsilateral to injection. A one-way ANOVA followed by Tukey's multiple comparison test was performed and differences regarded as significant when  $p < 0.05$ . \* Indicates significant different from control group.

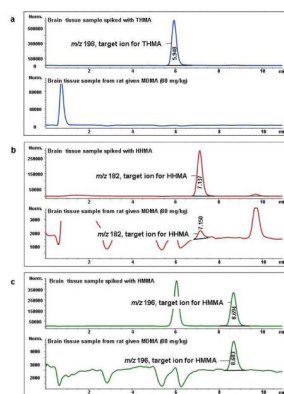


**Figure 3.** DA (upper panel) and DOPAC (lower panel) levels in striatum of rats one week after intracerebroventricular administration of THMA (1000 nmol). Control animals received unilateral intracerebroventricular injections of an equivalent volume of aCSF. Values represent the mean  $\pm$ SD. A one-way ANOVA followed by Tukey's multiple comparison test was performed and differences regarded as significant when  $p < 0.05$ . \* Indicates significant different from control group.



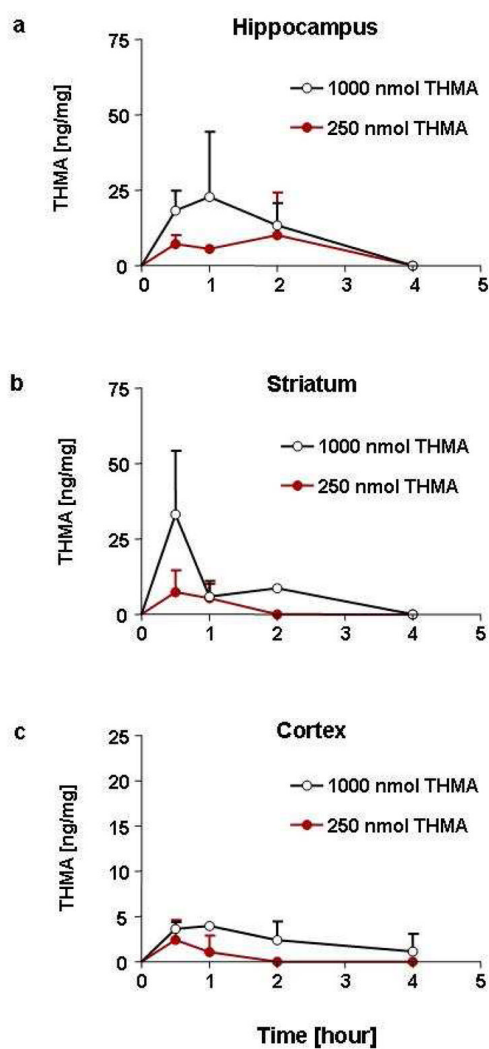
**Figure 4.**

Effect of fluoxetine on lasting deficits of 5HT and 5-HIAA after THMA. Shown are concentrations of 5-HT and 5-HIAA in the hippocampus of rats 1 week after drug administration in four different groups of animals. Rats were administered either aCSF or THMA (150  $\mu$ g) into the lateral ventricle. Rats were pre-treated with either saline or fluoxetine (10 mg/kg, i.p.) 65 and 5 min prior to the intracerebroventricular THMA injection. A one-way ANOVA followed by Tukey's test for multiple comparisons was used to test for significant differences among treatment groups. Differences were considered significant when  $p < 0.05$ . \* Indicates significant difference from the saline/aCSF group; \*\* indicates significant difference between the saline/THMA and fluoxetine/THMA group.

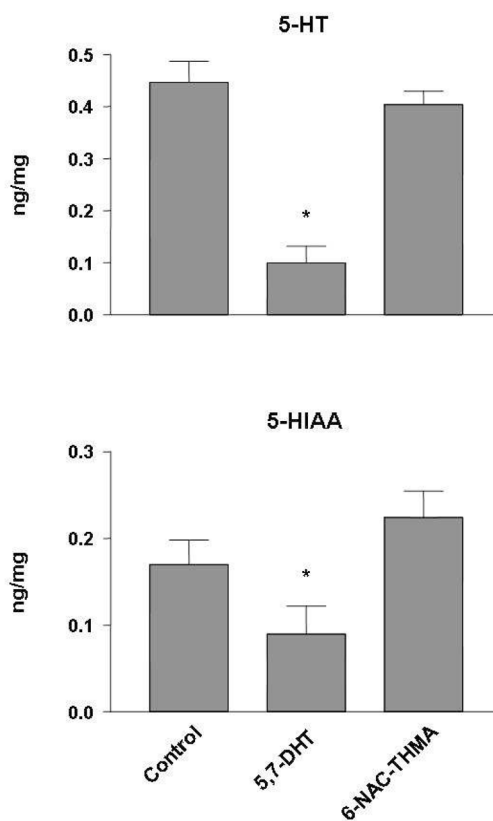


**Figure 5.**

Mass chromatograms of the target ions of THMA (a), HHMA (b), and HMMA (c). Top chromatograms of each part (a–c) show given ions in rat brain tissue spiked with THMA, HHMA, and HMMA, respectively. Final tissue concentration of each spiked analyte was 5  $\mu\text{g/g}$ . Bottom chromatograms of each part (a–c) show given ions in an authentic brain tissue samples taken from rats (N=3) treated with a high neurotoxic dose of MDMA (80 mg/kg; SC) three hours previously. Similar results were obtained in rats treated identically but sacrificed 1.5 (instead of 3) hr after drug administration.

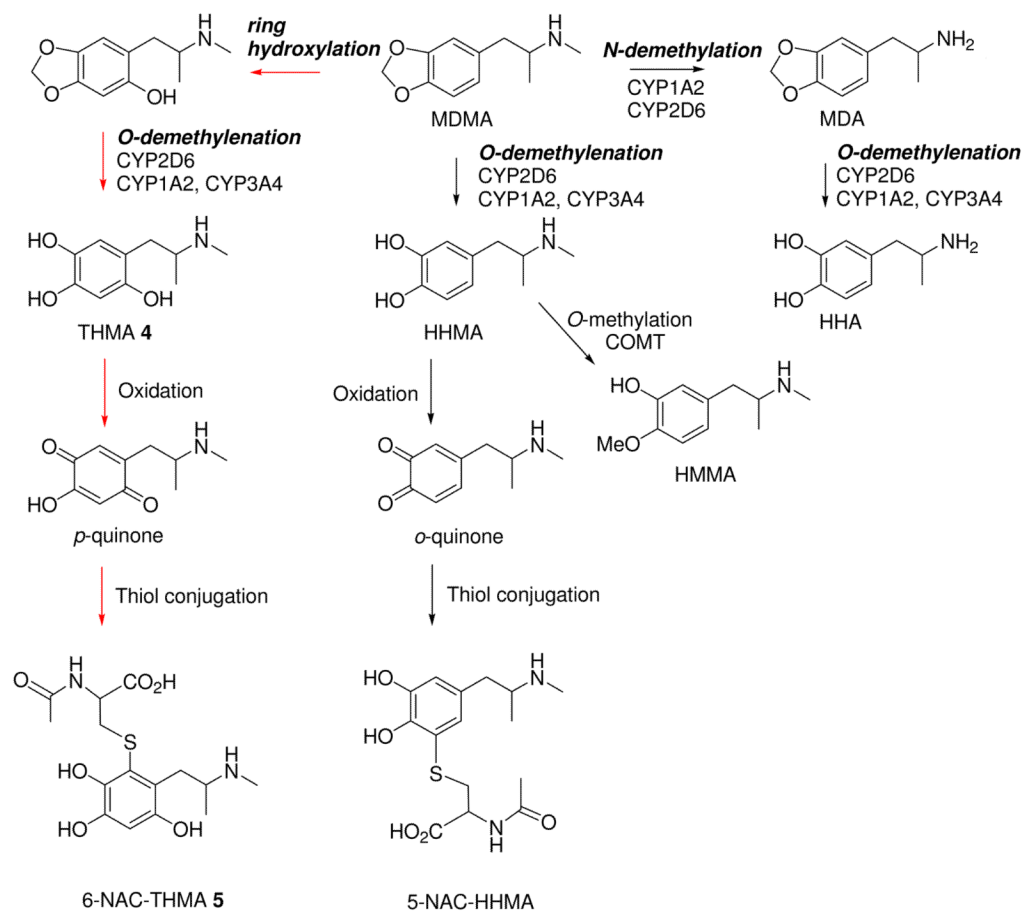


**Figure 6.** Concentrations of THMA in the ipsilateral hippocampus (a), striatum (b), and cerebral cortex (c) at various time points after intracerebroventricular administration of 250 or 1000 nmol of THMA. Values represent the mean  $\pm$ SD (N=3 rats at each time point).

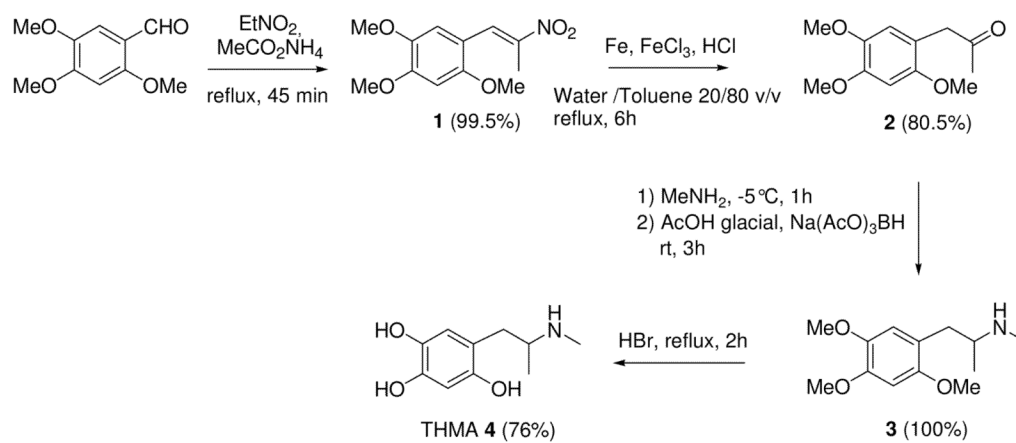


**Figure 7.**

5-HT levels and 5-HIAA levels in ipsilateral frontal cortex of rats two weeks after cortical administration of 42 nmol 6-NAC-THMA. The thioether conjugate was injected four times, with a 12-h interval between each injection. 6-NAC-THMA was dissolved in aCSF shortly before each injection. Control animals received unilateral intraparenchymal injections of an equivalent volume of aCSF. A positive control group consisted of animals that received a single intraparenchymal injection of 52 nmol of 5, 7-DHT. Values represent the mean  $\pm$ SD (N=8 in 6-NAC-THMA groups, N=6 in positive control groups, and N=6 in control groups). One-way ANOVA followed by Tukey's multiple comparison test was performed and differences regarded as significant when  $p < 0.05$ . \* Indicates significant different from control group.

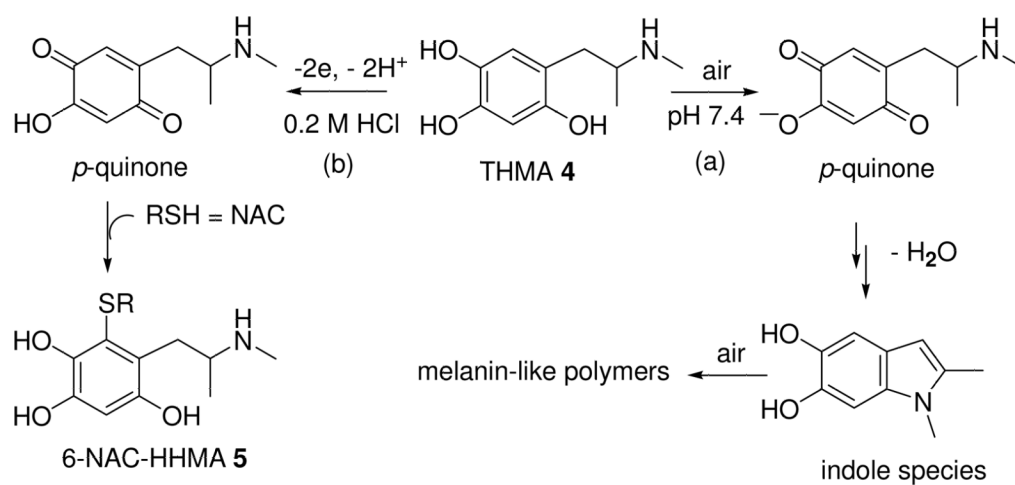
**Scheme 1.**

Metabolic pathways of MDMA along with the associated microsomal enzymes including the postulated conjugate formation; the numbered compounds correspond to the postulated metabolites synthesized and used for the biological experiments.



**Scheme 2.**  
Four Step Synthesis of THMA **4**



**Scheme 3.**

Oxidative polymerization of THMA 4 in pH 7.4 phosphate buffered aqueous solution under atmospheric conditions (path a); Two-step one-pot electrochemical synthesis of 6-NAC-HHMA 5 under acidic conditions (path b).